# Journal of Material Sciences & Engineering

**Research Article**  **OMICS International**

# Nanoparticle Shape and Thermal Radiation on Marangoni Water, Ethylene Glycol and Engine Oil Based Cu, Al$_2$O$_3$ and SWCNTs

**Nur Atikah Adnan, Kandasamy R\* and Mohammad R**

*Research Centre for Computational Fluid Dynamics, FSTPi, Universiti Tun Hussein Onn Malaysia, Malaysia, 86400, Batu Pahat, Johor, Malaysia*

## Abstract

The aim of this paper is to investigate the relationship between particle shape and radiation effects on Marangoni boundary layer flow and heat transfer of water, ethylene glycol and engine oil based Cu, Al$_2$O$_3$ and SWCNTs. There are three types of nanoparticle shapes are considered in this research such as sphere, cylinder and lamina. The governing nonlinear partial differential equations are reduced into a set of nonlinear ordinary differential equations by applying similarity transformation which is solved using shooting technique in conjunction with Newton's method and Runge Kutta algorithm. Temperature profiles are graphically and tabulary provided for the effects of solid volume fraction parameter, radiation parameter and empirical shape factor. The result shows that solid volume fraction and radiation energy gives a good impact on thermal boundary layer. Sphere nanoparticle shape predicts a better result on heat transfer rather than other nanoparticle shapes.

**Keywords:** Nanoparticle shape; Thermal radiation; Marangoni water; Ethylene glycol; Engine oil; Exponential temperature

## Introduction

Nanotechnology is one of widely technology rapidly progress in various fields such as chemistry, physics, materials science, biotechnology and other applications. It is due to their structures that are determined on the nanometer scale. It seems that Choi [1] is the first introduce term "nanofluids" for reference to base fluids suspended nanoparticles. Nanofluid is a fluid contains nanometer particles known as nanoparticles and made of metals, oxides, carbines or carbon nanotubes. The fluids are engineered colloidal suspension of nanoparticles in a base fluid. Water, ethylene glycol and oil are commonly example base fluid. Studies have shown that adding nanoparticles such as metal particles, metal oxides, metalloid oxides and carbon nanotubes, in the base fluids can effectively improve the thermal conductivity of the base fluids and enhance heat transfer performance of the liquid.

Studies have shown that nanofluid exhibit heat transfer characteristic compare to conventional fluid. There are several numerical and experimental studies on heat transfer in nanofluids: conductive, convective and radiative. Sidik et al. [2] presented an inclusive review on preparation methods and challenges of nanofluids. In addition, Pang et al. [3] presented the recent development and research effort of heat and mass transfer in nanofluid. Based on the research, most of the researchers are focusing on thermal conductivity and the heat transfer performance affected by the following parameters: nanoparticle material, nanoparticle size, nanoparticle shape, temperature and additives.

Marangoni boundary layer is the dissipative layer which may occur along the liquid-gas or liquid-liquid interfaces. Marangoni flow, occur at surface temperature gradient or the surface concentration gradient, appears in many practical projects such as chemical reaction process [4], aerospace engineering, crystal growth [5] and silicon melt [6]. There are two types of Marangoni which is thermal Marangoni effect (EMT) and solute Marangoni effect (EMS). Pearson [7] was introduced the mechanism of EMT.

The mechanism of thermal Marangoni effect (EMT) occur when a thin layer of fluid is heated from below and the temperature gradient is such that small variations in the surface temperature lead to surface tractions which cause the fluid to flow. Then, it tends to maintain the original temperature variations. Scriven and Sternling [8] are researchers who introduced the mechanism of EMS. Recently, there have been several papers published on the mechanism of Marangoni boundary layer flow transport. Christopher and Wang [9] present the effects of Prandtl number and Marangoni number on the Marangoni boundary layer around a vapor bubble during nucleation and growth by the shooting method.

In addition, Zheng et al. [10] examined the analytical result for Marangoni convection over a liquid-vapor surface due to an imposed temperature gradient by the Adomian decomposition technique couple with the Padé approximant technique. Then, Chamkha et al. [11] obtained a set of exact analytical results for the MHD thermosolutal Marangoni boundary layers over a flat surface. Later on, Chen [12] investigated the influence of Marangoni boundary layer on the flow and heat transfer of power-law fluids in a finite thin film over an unsteady stretching sheet.

Thus a research is carry out to investigate the relationship between particle shape and radiation effects on Marangoni boundary layer flow and heat transfer of copper, alumina and SWCNTs- water nanofluid, ethylene glycol and engine oil. There are three types of nanoparticle shapes are considered in this research such as sphere, cylinder and lamina. The governing nonlinear partial differential equations was reduced into a set of nonlinear ordinary differential equations by applying similarity transformation which are solved using shooting technique in conjunction with Newton's method and Runge Kutta algorithm. Temperature profiles are graphically and tabularly presented

**\*Corresponding author:** Ramasamy Kandasamy, Research Centre for Computational Fluid Dynamics, FSTPi, Universiti Tun Hussein Onn Malaysia, Malaysia, 86400, Batu Pahat, Johor, Malaysia, Tel: 006 07 453 7416; Fax: 006 07 453 6051; E-mail: ramasamy@uthm.edu.my

for the effects of solid volume fraction parameter, radiation parameter and empirical shape factor.

## Mathematical Analysis

The problem is consider as two dimensional steady Marangoni boundary layer flow and heat transfer of copper, alumina and SWCNTs in the presence of water, ethylene glycol and engine oil above a flat interface with surface tension gradient due to an exponential temperature. The physical model is assumed as incompressible, the base fluid and nanoparticle are in thermal equilibrium, no slippage and the flow is laminar.

Schematic of the physical system is shown in Figure 1 where Y is the coordinate measured normal to the surface whereas X axis pointing toward the porous medium. In addition, the thermo physical properties of the base fluid and nanoparticles copper, alumina and SWCNTs are given in Table 1 [13,14]. Marangoni effect acts as a boundary condition on the governing equations for the flow and it is unlike the Boussinesq effect in buoyancy-induced flow. The basic equations can be written in Cartesian coordinates X and Y as:

$$\frac{\partial U}{\partial X} + \frac{\partial V}{\partial Y} = 0 \tag{1}$$

$$U\frac{\partial U}{\partial X} + V\frac{\partial U}{\partial Y} = \frac{\mu_{nf}}{\rho_{nf}}\frac{\partial^2 U}{\partial Y^2} \tag{2}$$

$$U\frac{\partial T}{\partial X} + V\frac{\partial T}{\partial Y} = \alpha_{nf}\frac{\partial^2 T}{\partial Y^2} - \frac{1}{(\rho C_p)_{nf}}\frac{\partial q_r}{\partial Y} \tag{3}$$

The boundary conditions are

$$Y=0: \mu_{nf}\frac{\partial U}{\partial Y}\Big|_{Y=0} = \frac{\partial \sigma}{\partial X}\Big|_{Y=0} = 0, T\mid_{Y=0} = T_w = T_\infty + T_{const}e^{-X/L_0} \tag{4}$$

$$Y\to\infty: U\mid_{Y\to\infty} = 0, T\mid_{Y\to\infty} = T_\infty \tag{5}$$

Where U and V are the velocity components along the *X* and *Y* directions respectively. $M_{nf}$ is the viscosity of nanoparticle-nanofluid and $\rho_{nf}$ is the density of the nanofluid. *T* is temperature, $\alpha_{nf}$ is thermal
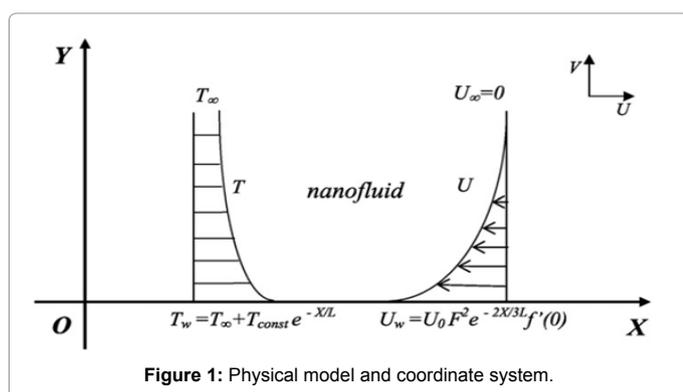


**Figure 1:** Physical model and coordinate system.

| | C$_p$ (J/kgK) | ρ (kg/m³) | k (W/Mk) |
|---|---|---|---|
| Cu | 385 | 8933 | 400 |
| Al$_2$O$_3$ | 765 | 3970 | 40 |
| SWCNTs | 425 | 2600 | 6600 |
| Water | 4179 | 997.1 | 0.613 |
| Ethylene glycol | 2430 | 1115 | 0.253 |
| Engine oil | 1910 | 884 | 0.144 |

**Table 1:** Thermo physical properties of Copper, Alumina and SWCNTs – water, ethylene glycol and engine oil.

diffusivity of the nanofluid, $c_p$ is specific heat at constant pressure, $(\rho c_p)_{nf}$ is heat capacity of the nanofluid and $q_r$ is the radiative heat flux. $T_w$ is surface temperature and it is assumed to be an exponential function with X, $T_\infty$ is the temperature of nanofluid far from the interface and $T_{const}$ is a reference temperature.

The others physical characteristics of the nanofluid are given by refs. [15,16].

$$\mu_{nf} = \frac{\mu_f}{(1-\varphi)^{2.5}} \tag{6}$$

$$\rho_{nf} = (1-\varphi)\rho_f + \varphi\rho_s \tag{7}$$

$$\alpha_{nf} = \frac{k_{nf}}{(\rho C_p)_{nf}}, \quad \gamma_{nf} = \frac{\mu_{nf}}{\rho_{nf}} \tag{8}$$

$$(\rho C_p)_{nf} = (1-\varphi)(\rho C_p)_f + \varphi(\rho C_p)_s \tag{9}$$

$\rho_{nf}$ is the density of water, $\rho_s$ is density of solid nanoparticles, $(\rho c_p)_f$ is the heat capacity of fluid $(\rho c_p)_s$ is the heat capacity of solid nanoparticles. $\gamma_{nf}$ is kinematic viscosity of nanofluid, $k_{nf}$ is thermal conductivity of nanofluid. In this research, the nanoparticles shapes are taken into account by using Hamilton and Crosser model [17].

$$\frac{K_{nf}}{K_f} = \frac{[k_s + (m-1)k_f] - (m-1)\varphi(k_f - k_s)}{[k_s + (m-1)k_f] + \varphi(k_f - k_s)} \tag{10}$$

where $k_f$ is thermal conductivity of nanofluid, $k_s$ is thermal conductivity of solid nanoparticles, $m=3/\varphi$ is empirical shape factor where $\varphi$ is sphericity. By using Rosseland approximation, the radiative of heat flux is become to:

$$q_r = -\frac{4\delta^*}{3k^*}\frac{\partial T^4}{\partial Y} \tag{11}$$

where $k^*$ is the mean absorption and $\delta^*$ is Stefan Boltzman. The temperature on the surface is an exponential function with X. Moreover, there are temperature differences within the flow; $T^4$ is expressed as a linear function of temperature. This accomplished by expanding $T^4$ in a Taylor series about T∞. The higher-order terms are neglecting, thus it become:

$$T^4 \approx 4T_\infty^3 T - 3T_\infty^4 \tag{12}$$

According to the boundary condition 4, $\sigma$ is defined as surface tension. The temperature gradient occur by interfacial surface tension gradient at the interface induced flow as

$$\frac{\partial \sigma}{\partial X} = \frac{\partial \sigma}{\partial T} \cdot \frac{\partial T}{\partial X} \tag{13}$$

In addition, it is assumed that the surface tension is linear with the temperature such that

$$\sigma = \sigma_0 - \gamma_T(T - T_\infty), \gamma_T = -\frac{\partial \sigma}{\partial T} \tag{14}$$

$\sigma_0$ is a positive constant and it represents the surface tension when $T=T_\infty$. $\gamma_T$ is the temperature coefficient of the surface tension. We introduced the similar dimensionless variables ($U_0$ is velocity unit, $L_0$ is length unit):

$$u = \frac{U}{U_0}, v = \frac{V}{U_0}\left(\frac{U_0 L_0}{\gamma_f}\right)^{\frac{1}{2}} = \frac{v}{U_0}\mathrm{Re}^{\frac{1}{2}} \tag{15}$$

$$x = \frac{X}{L_0}, y = \frac{Y}{L_0}\left(\frac{U_0 L_0}{\gamma_f}\right)^{\frac{1}{2}} = \frac{Y}{L_0}\mathrm{Re}^{\frac{1}{2}} \tag{16}$$

$$t = \frac{T}{T_\infty} \qquad (17)$$

$$a = (1-\varphi)^{2.5}\left[(1-\varphi)+\varphi\frac{\rho_s}{\rho_f}\right] \qquad (18a)$$

$$b = \left[(1-\varphi)+\varphi\frac{(\rho C_p)_s}{(\rho C_p)_f}\right]\frac{[k_s+(m-1)k_f]-(m-1)\varphi(k_f-k_s)}{[k_s+(m-1)k_f]+\varphi(k_f-k_s)} \qquad (18b)$$

$$= (\quad - \quad)^{2.5} \qquad (18c)$$

$$\mathrm{Re}=\frac{U_0L_0}{\gamma_f},\mathrm{Pr}=\frac{\gamma_f}{\alpha_f},\gamma_f=\frac{\mu_f}{\rho_f},Ma=\frac{\gamma_TT_{const}L_0}{\mu_f\alpha_f},Nr=\frac{16\delta^*T_\infty^3}{3k_{nf}k^*} \qquad (19)$$

Where $R_e$ is Reynolds number, $P_r$ is Prandtl number. In this paper, we consider $P_r=7.8$ and Ma is Marangoni number and Nr is the radiation parameter. So, the governing eqns. (1)-(3) can be transformed to:

$$\frac{\partial u}{\partial x}+\frac{\partial v}{\partial y}=0 \qquad (20)$$

$$u\frac{\partial u}{\partial x}+v\frac{\partial u}{\partial y}=\frac{1}{a}\frac{\partial^2 u}{\partial y^2} \qquad (21)$$

$$u\frac{\partial t}{\partial x}+v\frac{\partial t}{\partial y}=\frac{1+Nr}{b\,\mathrm{Pr}}\frac{\partial^2 t}{\partial y^2} \qquad (22)$$

Boundary conditions (4)-(5) become:

$$y=0:\frac{T_{const}}{T_\infty}\frac{\partial u}{\partial y}\bigg|_{y=0}=-\frac{Ma}{\mathrm{Pr}}\left(\frac{1}{\mathrm{Re}}\right)^{\frac{3}{2}}c\frac{\partial t}{\partial x}\bigg|_{y=0},v=0,t\,|_{y=0}=1+\frac{T_{const}}{T_\infty}e^{-x} \quad (23)$$

$$y\to\infty:u\,|_{y\to\infty}=0,t\,|_{y\to\infty}=1 \qquad (24)$$

Using the boundary layer approximation and introducing the stream function $\psi$ defined as $u=\frac{\partial\psi}{\partial y}$ and $v=\frac{\partial\psi}{\partial y}$, the following transformation variables are:

$$\psi(x,y)=Fe^{\frac{-x}{3}}f(\eta),\eta=Fe^{\frac{-x}{3}}y,F=\left(\frac{Ma}{\mathrm{Pr}}\right)^{\frac{1}{3}}\left(\frac{1}{\mathrm{Re}}\right)^{\frac{1}{2}} \qquad (25)$$

$$t(x,y)=1+\frac{T_{const}}{T_\infty}e^{-x}\theta(\eta) \qquad (26)$$

The partial differential eqns. (20)-(22) are transformed to the following ordinary equations:

$$f'''(\eta)=a\left[\frac{1}{3}f(\eta)f''(\eta)-\frac{2}{3}f'(\eta)^2\right] \qquad (27)$$

$$\theta''(\eta)=\frac{b\,\mathrm{Pr}}{1+Nr}\left[\frac{1}{3}f(\eta)\theta'(\eta)-f'(\eta)\theta(\eta)\right] \qquad (28)$$

Boundary conditions (23)-(24) can be expressed as

$$f(0)=0,f''(0)=c,f'(\infty)=0 \qquad (29)$$

$$\theta(0)=1,\theta(\infty)=0 \qquad (30)$$

The X and Y component of the velocity and temperature are:

$$U=U_0\left(\frac{Ma}{\mathrm{Pr}}\right)^{\frac{2}{3}}\frac{1}{\mathrm{Re}}e^{\frac{-2x}{3L_0}}f'(\eta)=\left(\frac{\gamma_TT_{const}\gamma_f}{\rho_fL_0^2}\right)^{\frac{2}{3}}\frac{\mathrm{Re}}{U_0}e^{\frac{-2x}{3L_0}}f'(\eta) \qquad (31)$$

$$V=\frac{1}{3}\left(\frac{\gamma_TT_{const}\gamma_f}{\rho_fL_0^2}\right)^{\frac{1}{3}}e^{\frac{-x}{3L_0}}\left[f(\eta)+\eta f'(\eta)\right] \qquad (32)$$

$$T=T_\infty+T_{const}e^{\frac{-x}{L_0}}\theta(\eta) \qquad (33)$$

Local Nusselt number $Nu_x$ defined as:

$$Nu_x=\frac{xq_w(x)}{k(T)\left[T(X,0)-T(X,\infty)\right]} \qquad (34)$$

$q_w(X)$ is heat flux of nanofluid as $q_w(X)=-k(T)\left(\frac{\partial T}{\partial Y}\right)\big|_{y=0}$. By using eqns. (25), (26), (33) and (34) (Table 2 and Figure 2),

$$Nu_x=-\frac{X}{L_0}e^{\frac{-x}{3L_0}}\left(\frac{\gamma_T^2T_{const}^2}{\rho_f^2U_0^3L_0\gamma_f}\right)^{\frac{1}{6}}\theta'(0) \qquad (35)$$

## Numerical Techniques

The set of nonlinear ordinary differential eqns. (27) and (28) with boundary condition (29-30) are reduced to the first order differential equations and have been solved by using Runge Kutta scheme in conjunction with modified Newton- Raphson shooting method .The terms in eqns. (27) and (29) are expressed as a set of first order equations in terms of three variables $u$, $v$ and $r$. Introducing the shooting parameter $t$ as $f'(0)=t$ and $f(\eta)$, $f'(\eta)$ and $f''(\eta)$ are denoting by using variables $u$, $v$ and $r$ yields:

$$\begin{aligned}
&f=f(\eta)\\
&f'=\frac{d}{d\eta}f(\eta)=u(\eta)\\
&f''=\frac{d^2}{d\eta^2}f(\eta)=\frac{d}{d\eta}u(\eta)=v(\eta)\\
&f'''=\frac{d^3}{d\eta^3}f(\eta)=a(f(\eta).v(\eta)-2u(\eta)^2)/3
\end{aligned} \qquad (36)$$

$$f(0)=0,\quad u(0)=t,\quad v(0)=c \qquad (37)$$

Then the eqns. (27) and (28) can be converted into

$$diff(v(\eta),\eta)-a.\left(\left(\frac{1}{3}\right).f(\eta).v(\eta)-\left(\frac{2}{3}\right).u(\eta)^2\right) \qquad (38)$$

$$diff(r(\eta),\eta)-\left(b.\frac{(\mathrm{Pr})}{(1+q)}\right).\left(\left(\frac{1}{3}\right).f(\eta).r(\eta)-u(\eta).\theta(\eta)\right) \qquad (39)$$

The asymptotic boundary conditions $\infty$ given in eqns. (29) and (30) were replaced by a finite value of 8 for similarity variable $\eta$ maximum as follows:

$$u(8)=0\quad v(8)=1\quad \theta(8)=0 \qquad (40)$$

|   | Sphere | Cylinder | Lamina |
|---|--------|----------|--------|
| $\varphi$ | 1 | 0.4710 | 0.1857 |
| $m$ | 3 | 6.3698 | 16.1576 |

**Table 2:** Values of the sphericity and the empirical shape factor for different particles shapes.
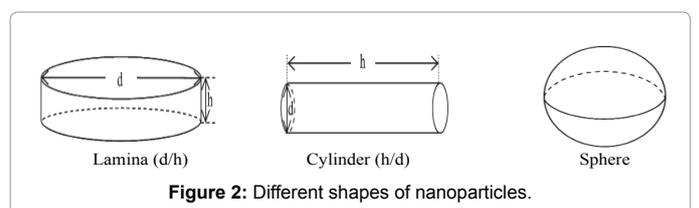


**Figure 2:** Different shapes of nanoparticles.

MAPLE 18 software for fourth fifth order Runge Kutta method is using to find the values of heat transfer and velocity.

## Results and Discussion

In this research, Marangoni boundary layer flow and heat transfer of nanoparticle shapes (sphere, cylinder and lamina) in the presence of water; ethylene glycol and engine oil based on copper, alumina and SWCNTs are investigated by exponential temperature. Organization the rate of heat transfer and temperature within the nanofluid with different nanoparticle shapes are observed in terms of figures and tables where the influences of the solid volume fraction, radiation parameter and empirical shape factor are considered.

## Analysis of nanoparticle shape and volume fraction on temperature profiles

The solid volume fraction is an important component in the physical parameter for nanofluids and plays a key role in Marangoni boundary layer flow and heat transfer. The academic literature [18,19] had revealed that the solid volume fraction on copper-water nanofluid in the range $0.05\% \leq \phi \leq 6.00\%$. If the concentration is exceeds 6.00%, the sendimation would take place. In this study, the solid volume fraction parameter consider as $\phi$=0.0%, 0.1% and 0.2% while the others physical parameters are fixed as Pr=7.8, Nr=1 and m=3 (sphere particle), m=6.3698 (cylinder particle) and m=16.1576 (lamina particle). Figure 3
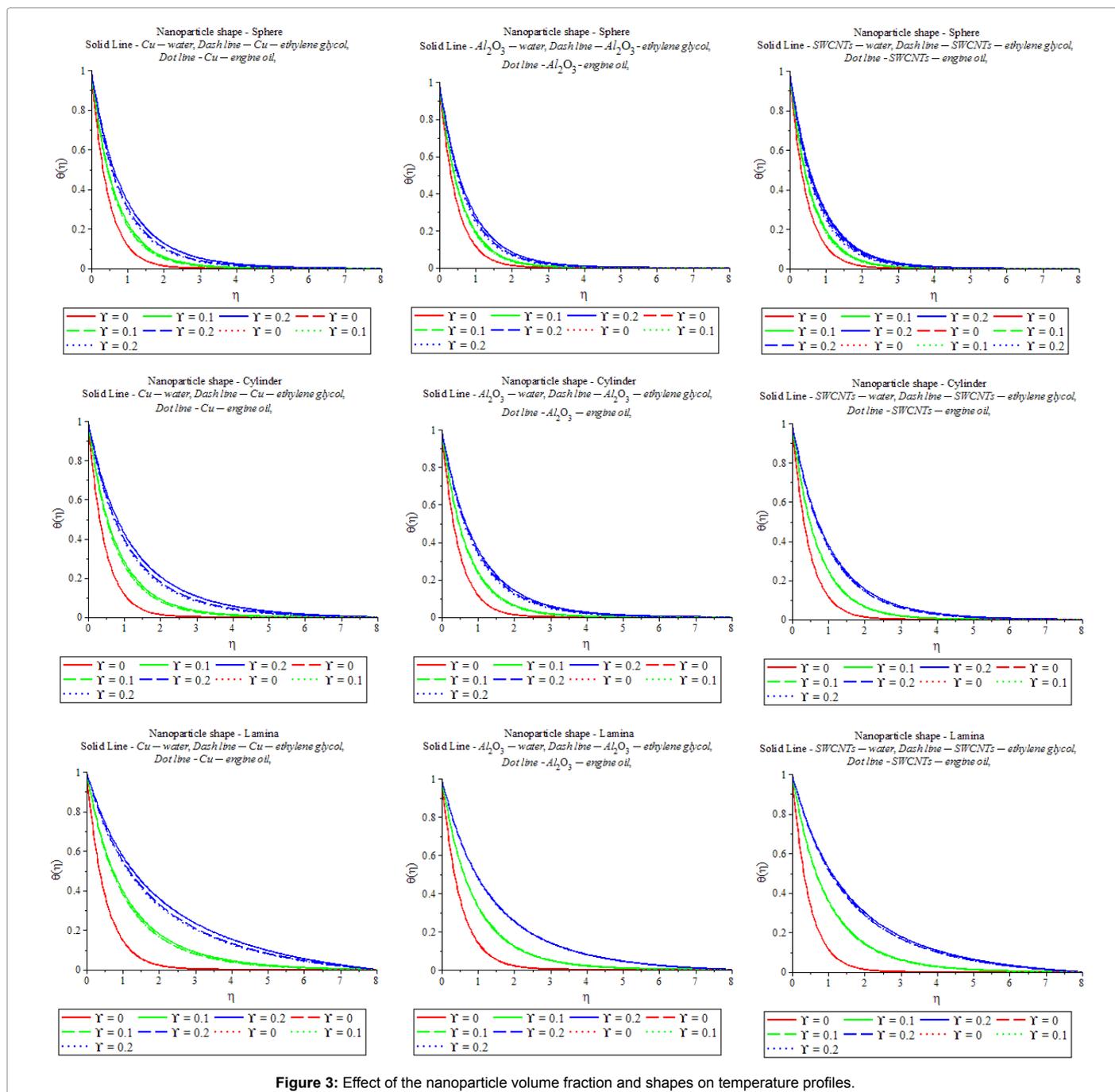


**Figure 3:** Effect of the nanoparticle volume fraction and shapes on temperature profiles.

displays the effects of solid volume fraction parameter on heat transfer of the water, ethylene glycol and engine oil Cu, Al$_2$O$_3$ and SWCNTs for sphere, cylinder and lamina particles.

It is already known that Marangoni effect on fluid flow is fluid moves from a region with low surface tension to a region with high surface tension. It is observed that the temperature of the water, ethylene glycol and engine oil based Cu, Al$_2$O$_3$ and SWCNTs increases with increase of nanoparticle volume fraction. The outcomes of the investigation shows that the thermal boundary layer thickness of sphere shape copper nanoparticles in Cu-water is stronger than that of all the other mixtures in the flow regime. This is due to the combined effects of the density and thermal conductivity of the Cu-water is more significant as compared to the other mixtures in the flow regime.

### Analysis of the radiation and nanoparticle shape on temperature profiles

Figures displays the results obtained from the influence of the thermal radiation energy on heat transfer characteristic of the water ethylene glycol and engine oil based Cu, Al$_2$O$_3$ and SWCNTs on dimensionless temperature $\theta$ ($\eta$). As shown in the Figure 4, the dimensionless temperature of the water ethylene glycol and engine oil based Cu, Al$_2$O$_3$ and SWCNTs increases with increase of thermal
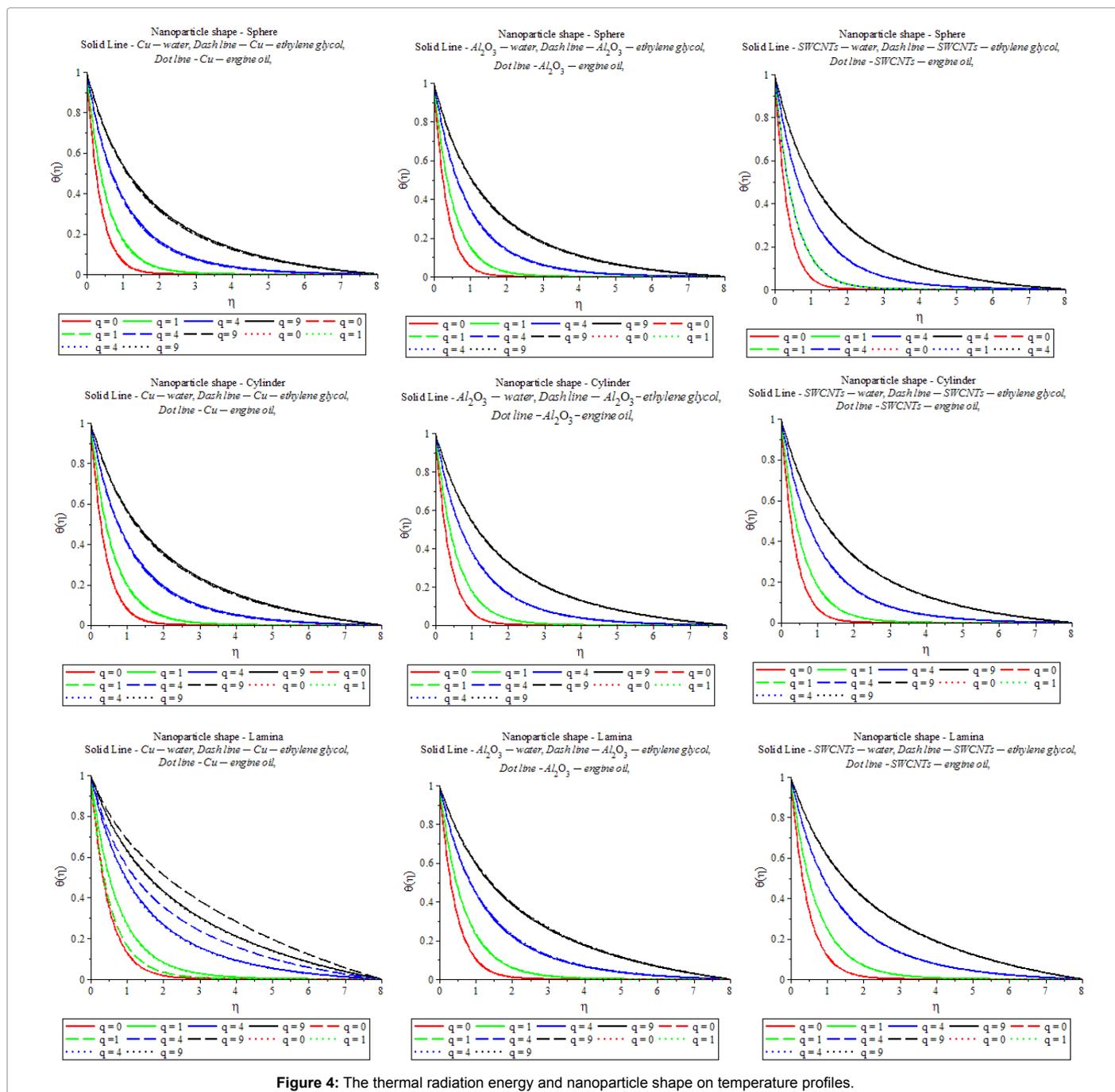


**Figure 4:** The thermal radiation energy and nanoparticle shape on temperature profiles.

radiation energy. It is because presence of radiation to put off the repairing effect of thermal Marangoni boundary layer. Besides that the temperature distribution within the thermal boundary layer invert to $T_\infty$ slowly. It is interesting to notice that the thermal boundary layer thickness of the lamina shape Cu - ethylene glycol is more powerful as compared to the other mixtures in the flow regime with increase of thermal radiation energy because of the combined effect of thermal conductivity and the specific heat of the Cu - ethylene glycol along the flow. What stand out in the Figure 4 is lamina shape copper nanoparticles in ethylene glycol leads an efficient hits on temperature distribution with increase of thermal radiation energy.

### Effect of the empirical shape factor (m)

Nanoparticle shape is another significant aspect on flow and heat transfer of nanofluid. Most of the researchers investigating nanofluid have utilized spherical shape because it's effective thermal conductivity. Thermal conductivity of nanofluids can be approximated by Hamilton and Crosser model as $\frac{K_{nf}}{K_f} = \frac{[k_s + (m-1)k_f] - (m-1)\varphi(k_f - k_s)}{[k_s + (m-1)k_f] + \varphi(k_f - k_s)}$ where the sphericity and empirical shape factor ($m$) are considered. In this study, three types of nanoparticle shapes are taken into account such as sphere, cylinder and lamina.

Different shapes of copper, alumina and SWCNTs particles are presented in Figure 2 and empirical shape factor are derived in Table 1. According to Figure 2, $N$ is height and diameter ratio of cylinder defined as $N=h/d$ where $h$ is height of the cylinder and $d$ is the diameter. The empirical shape factor and the sphericity of a cylinder can be expressed by:

$$m(N) = \frac{2N+1}{2N}\sqrt[3]{12N}, \phi(N) = \frac{2N}{2N+1}\sqrt[3]{\frac{9}{4N}} \qquad (41)$$

There is a differentiation between cylinder and lamina. Cylinder is defined as a column for $N \geq 10$ whereas lamina is defined for $N \leq 0.1$.

Figure 5 displays an overview influence of different type's nanoparticle shapes (sphere, cylinder lamina) on dimensionless temperature of the water, ethylene glycol and engine oil based Cu, Al₂O₃ and SWCNTs. The results show that for different nanoparticle shapes with the same base fluid and other parameters, the dimensionless temperature is sphere<cylinder<lamina. Meanwhile, the rate of temperature is decreases sphere>cylinder>lamina. According to the result, it is indicated that the sphere shape nanoparticles in the water

Cu, Al₂O₃ and SWCNTs plays a dominant role as compared with the other mixtures in the flow regime.

The results of this investigation show that nanoparticle volume fraction and particle shape give a significant impact on thermal conductivity of the copper, alumina and SWCNTs. The ratio thermal of conductivity is increases as solid volume fraction increases for the same particle shape (sphere, cylinder and lamina) in the presence of water, ethylene glycol and engine oil based on Cu, Al₂O₃ and SWCNTs. In addition, thermal conductivity increases when sphericity $\varphi(N)$ increases or empirical shape factor $m(N)$ decreases in the same solid volume fraction. In sequence order, the ratio thermal conductivity is sphere<cylinder<lamina. These results are similar to Jiao et al. [19].

## Conclusion

The present study was designed to determine the effect of particle shapes and radiation parameter on Marangoni boundary layer flow and heat transfer of copper, alumina and SWCNTs in the presence of water, ethylene glycol and engine oil driven by exponential temperature. The following results are obtained:

1. There is a positive significant correlation between nanoparticle volume fraction parameter and particle shape on temperature and thermal conductivity.

2. The sphere shape nanoparticles in the presence of water Cu, Al₂O₃ and SWCNTs play a dominant role as compared with the other mixtures in the flow regime.

3. Sphere shape nanoparticles in the nanofluid is a more assurance in terms of enhancing the heat transfer compared to other nanoparticles shapes.

4. Lamina shape copper nanoparticles in ethylene glycol leads an efficient hit on temperature distribution with increase of thermal radiation energy.

5. The thermal boundary layer thickness of sphere shape copper nanoparticles in Cu-water is stronger than that of all the other mixtures in the flow regime because of the thermal conductivity of Cu - water.

It is registered that the lamina shape nanoparticle in the existence of Cu-ethylene glycol is researched in this work can be gainful in the solar radiation energy systems. Resultantly, the lamina shape in the cu-ethylene glycol is a more affirmation in terms of complementing
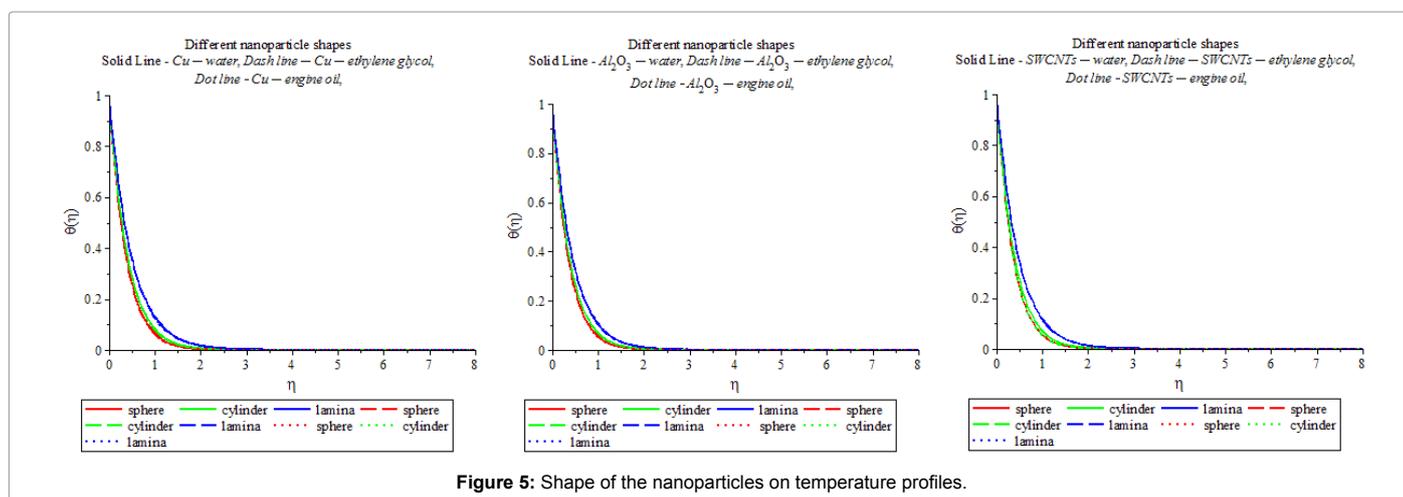


**Figure 5:** Shape of the nanoparticles on temperature profiles.

the heat transfer reinforcement of the Marangoni boundary layer flow system.

## References

1. Chol SUS (1995) Enhancing thermal conductivity of fluids with nanoparticles. ASME-Publications-Fed 231: 99-106.

2. Sidik NAC, Mohammed HA, Alawi OA, Samion S (2014) A review on preparation methods and challenges of nanofluids. International Communications in Heat and Mass Transfer 54: 115-125.

3. Pang C, Lee JW, Kang YT (2015) Review on combined heat and mass transfer characteristics in nanofluids. International Journal of Thermal Sciences 87: 49-67.

4. Zhang Y, Zheng L (2012) Analysis of MHD thermosolutal Marangoni convection with the heat generation and a first-order chemical reaction. Chemical engineering science 69: 449-455.

5. Arafune K, Hirata A (1999) Thermal and solutal Marangoni convection in In–Ga–Sb system. Journal of Crystal Growth 197: 811-817.

6. Li J, Li M, Hu W, Zeng D (2003) Suppression of Marangoni convection of silicon melt by a non-contaminating method. International journal of heat and mass transfer 46: 4969-4973.

7. Pearson JRA (1958) On convection cells induced by surface tension. Journal of fluid mechanics 4: 489-500.

8. Scriven LE, Sternling CV (1960) The marangoni effects. Nature 187: 186-188.

9. Christopher DM, Wang B (2001) Prandtl number effects for Marangoni convection over a flat surface. International Journal of Thermal Sciences 40: 564-570.

10. Zheng L, Zhang X, Gao Y (2008) Analytical solution for Marangoni convection over a liquid–vapor surface due to an imposed temperature gradient. Mathematical and Computer Modelling 48: 1787-1795.

11. Al-Mudhaf A, Chamkha AJ (2005) Similarity solutions for MHD thermosolutal Marangoni convection over a flat surface in the presence of heat generation or absorption effects. Heat and Mass Transfer 42: 112-121.

12. Chen CH (2007) Marangoni effects on forced convection of power-law liquids in a thin film over a stretching surface. Physics Letters A 370: 51-57.

13. Malvandi A, Hedayati F, Ganji DD (2014) Slip effects on unsteady stagnation point flow of a nanofluid over a stretching sheet. Powder Technology 253: 377-384.

14. Sheikholeslami M, Ganji DD, Ashorynejad HR (2013) Investigation of squeezing unsteady nanofluid flow using ADM. Powder Technology 239: 259-265.

15. Sheikholeslami M, Gorji-Bandpy M, Ganji DD, Soleimani S (2013) Effect of a magnetic field on natural convection in an inclined half-annulus enclosure filled with Cu–water nanofluid using CVFEM. Advanced Powder Technology 24: 980-991.

16. Kang HU, Kim SH, Oh JM (2006) Estimation of thermal conductivity of nanofluid using experimental effective particle volume. Experimental Heat Transfer 19: 181-191.

17. Sourtiji E, Gorji-Bandpy M, Ganji DD, Hosseinizadeh SF (2014) Numerical analysis of mixed convection heat transfer of Al2O3-water nanofluid in a ventilated cavity considering different positions of the outlet port. Powder Technology 262: 71-81.

18. Sourtiji E, Ganji DD, Seyyedi SM (2015) Free convection heat transfer and fluid flow of Cu–water nanofluids inside a triangular–cylindrical annulus. Powder Technology 277: 1-10.

19. Jiao C, Zheng L, Lin Y, Ma L, Chen G (2016) Marangoni abnormal convection heat transfer of power-law fluid driven by temperature gradient in porous medium with heat generation. International Journal of Heat and Mass Transfer 92: 700-707.